ADVANCED MATERIALS
www.advmat.de

www.MaterialsViews.com

On-Chip Manipulation of Protein-Coated Magnetic Beads via Domain-Wall Conduits

By *Marco Donolato, Paolo Vavassori, Marco Gobbi, Maria Deryabina, Mikkel F. Hansen, Vitali Metlushko, Bojan Ilic, Matteo Cantoni, Daniela Petti, Stefano Brivio,* and *Riccardo Bertacco**

Magnetic beads with functionalized surfaces are widely used as molecule carriers or labels for single molecule studies,[1] cell manipulation,[2] and biomagnetic sensing.[3] For this reason manipulation at the nanoscale of surface functionalized magnetic beads in suspension is of paramount importance in biotechnology, nanochemistry, and nanomedicine as it leads to a precise control of the tagged biological entity.

In the past few years many approaches have been developed both for the manipulation and transport of a massive particle population or of a single particle, e.g., microfabricated current-carrying wires,[4] micromagnets,[5] and magnetic tweezers.[6] More recently, thin films patterned into arrays of magnetic elements have also been proposed for the transport of single magnetic particles by exploiting their capability of focusing external magnetic fields.[7–9]

In addition, it has been shown that a fixed periodic landscape of magnetic domain walls (DWs) in a ferromagnetic thin film can be used to manipulate magnetic micro-particles at a solid-fluid interface.[10,11] However none of these techniques combines 2D translation, rotation, and trapping of single magnetic particles along multiple trajectories with a control at the micro- and nanoscale and compatibility with lab-on-chip applications, which are the most prominent features of our approach based on magnetic strips presented in this paper.

We demonstrate here the manipulation of individual micro- and nanobeads carrying proteins through the control of the motion of geometrically constrained DWs in magnetic nanoconduits patterned on the chip surface by means of a remote and low strength magnetic field.[12] Magnetic beads are conveyed on the chip surface through a microfluidic channel and then captured by the stray field of a DW; their capture, transport and release is obtained via precise control over DW nucleation, displacement, and annihilation processes in a DW conduit structure. As a specific demonstration of biological application of our approach, we show that different proteins previously immobilized on the surface of microbeads can be singularly transported along a DW conduit, or complexes of two beads carrying proteins with high chemical affinity can be created and then manipulated on the same structure. By simply designing the shape of the DW conduit it is possible to manipulate a particle along the desired path on the chip surface, with the precision of 100 nm, as we demonstrated for circular conduits. These results demonstrate the great potential of our approach for realizing sophisticated biological experiments involving small volumes of samples in a lab-on-a-chip system, essentially consisting in controlled biochemical analysis and synthesis.

In nanoscale ferromagnetic strips, shape anisotropy restricts the magnetization to lie parallel to the strip axis. Each magnetic domain has a head (positive or north pole) and a tail (negative or south pole). The resulting DWs are therefore either head-to-head (HH) or tail-to-tail (TT), and successive DWs along the nanostrip alternate between HH and TT configurations. These geometrically confined DWs exhibit intriguing properties and have become recently the focus of wide-spread theoretical[13,14] and experimental[15–19] research. Due to the geometrical confinement, the spin structure of a DW can be controlled via the lateral dimensions and film thickness of the nanostrip, while the DW size is on the order of tens of nm. Such DWs are ''spin blocks'' that behave as quasi-particles, which can be precisely manipulated by playing with external fields, spin-polarized currents[20–22] and geometry. In particular, variations of the geometry such as constrictions, protrusions or corners, can be used to shape the potential landscape for the DW in order to obtain a finely controlled manipulation of the DW displacement. In addition it has been shown that DWs can be propagated through complex 2D and 3D networks of nanostrips that contain bifurcation and intersection points.[23] All these peculiar properties have led to

[*] Prof. R. Bertacco, M. Donolato, M. Gobbi, Dr. M. Cantoni, D. Petti, S. Brivio
LNESS – Dipartimento di Fisica Politecnico di Milano
Via Anzani 42, I-22100 Como (Italy)
E-mail: riccardo.bertacco@polimi.it
Dr. P. Vavassori
CIC nanoGUNE Consolider, Tolosa hiribidea 76
ES-20018 Donostia-San Sebastian (Spain)
Dr. P. Vavassori
CNR-INFM S3, CNISM and Dipartimento di Fisica
Università di Ferrara
I-44100 Ferrara (Italy)
Dr. M. Deryabina, Prof. M. F. Hansen
Department of Micro- and Nanotechnology
DTU Nanotech
Technical University of Denmark
Building 345 East
DK-2800 Kongens Lyngby (Denmark)
Dr. B. Ilic
Cornell Nanofabrication Facility, Cornell University
Ithaca NY 14853 (USA)
Prof. V. Metlushko
Department of Electrical and Computer Engineering
University of Illinois at Chicago
Chicago IL 60607 (USA)

DOI: 10.1002/adma.201000146

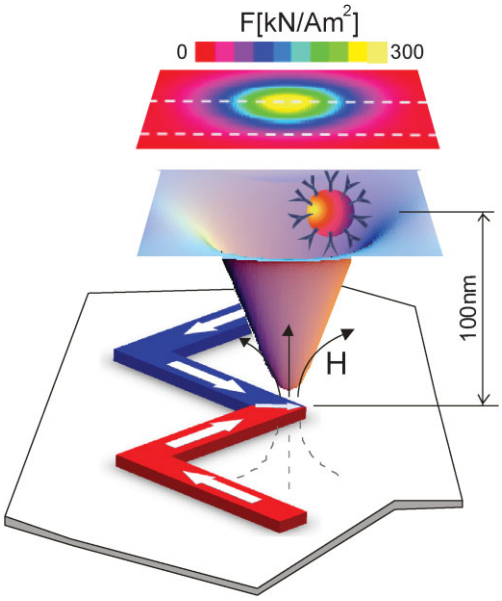

Figure 1. Bottom: sketch of a Py nanostrip with a DW in a corner and of the corresponding potential energy surface for a magnetic bead carrying antibodies on a plane at 100 nm from the Py structure. Top: color intensity plot of the modulus of the attractive force per unit magnetic moment.

many proposed nanowire based devices that have been intensively researched, prominent examples being random access memory[15] and logic devices.[23]

In this Communication, we present a novel intriguing application of DW motion in nanostrips, based on the coupling between the magnetic field of the DW and the magnetic moment of the bead. The basic ingredient of the application described here is the highly inhomogeneous magnetic stray field generated by a DW, of up to several kOe, which can trap a magnetic particle. This stray field is spatially localized at the nanometer scale due to the DW's very confined geometric structure. In Figure 1, the color intensity plot of the modulus of the attractive force together with a sketch of the potential energy surface experienced by a point magnetic dipole placed on a plane at 100 nm from the upper surface of a strip are presented. Both plots have been obtained by computing, with OOMMF, the magnetic field H created in the surrounding space by the HH DW and using the following vector expression for the force: $F = \mu_0(\mu \bullet \nabla)$ H, where μ is a unit magnetic moment ($\mu = 1\,A\,m^2$) placed in a plane at 100 nm from the nanowire surface. A typical value of μ of commercially available superparamagnetic nanoparticles employed in this work is on the order of 10^{-14}–$10^{-15}\,A\,m^2$, in which case the intensity of the attractive force can be estimated to be in the 0.1–1 nN range in a plane 100 nm above the conduit. The gradient of the magnetic stray field generated by the DW results in an attractive force, which tends to capture[25–28] and drag any magnetic particle in proximity of the DW as the DW moves.

In Figure 2 (top) we show the scanning electron microscopy (SEM) image of a zig-zag strip of Permalloy (Py) designed to implement an example of a controllable magnetic DW step motor that can be used to displace magnetic beads over large distances. The structure is prepared in a fully saturated initial state (Fig. 2a) by applying a saturating field H_0 of 500 Oe as indicated in the Figure. Subsequently the wider nucleation pad at the left-hand side of the strip is used for the nucleation of a reversed domain by applying a magnetic field H_i of 100 Oe as sketched in Figure 2. Since the pad is wider than the wire, a reversed domain nucleates there at lower fields than elsewhere. This results in the injection into the strip of a HH DW that propagates to the first bend in the zig-zag, acting as a pinning site (Fig. 2b). The H_i field is removed and a sequence of fields H_{up} and H_{dw} of 150 Oe can be applied as sketched in Figure 2 in order to displace the DW along each segment and, thus, throughout the entire conduit (Fig. 2c–e).

A zig-zag nanowire similar to that in Figure 2, but 30 μm long and covered with a 70-nm SiO_2 protecting layer, has been used to separately transport magnetic beads coated with streptavidin (Dynabeads MyOne, 1 μm diameter, Invitrogen), protein A and fluorescent antibodies (anti-streptavidin-Cy3) (Dynabeads Protein A, 2.8 μm diameter, Invitrogen), as well as pairs of beads bound by chemical affinity between streptavidin and fluorescent antibodies. The latter experiment is particularly relevant because it demonstrates the possibility of manipulating two interacting proteins initially carried by different beads, and has been chosen for illustrating the potential of the method. Note that micron sized beads have been used only because the investigation of their motion with a high speed camera coupled to an optical microscope is easier, but the method can be applied to "true" nanoparticles with diameter below 100 nm (see ref. [25] for the demonstration of capture of 80 nm nanoparticles in suspension by a DW).

The manipulation of single beads carrying only one protein will be described afterwards (see the movie M2). In order to avoid

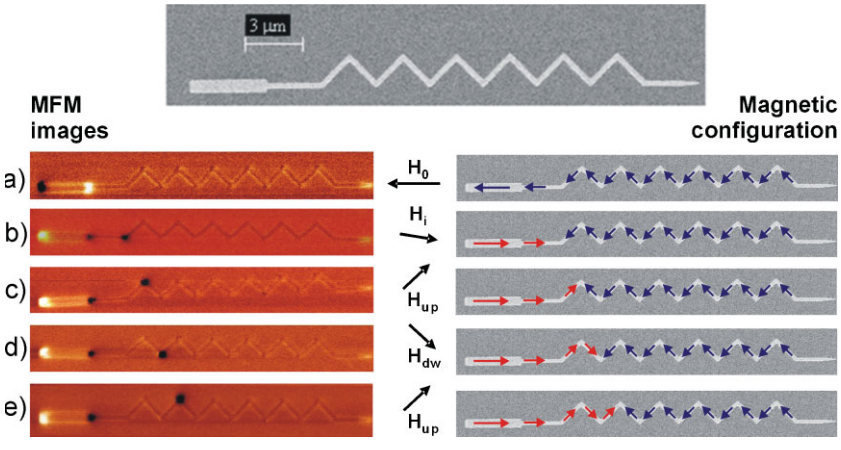

Figure 2. Top: SEM image of the zig-zag wire structure made of Py used to implement a controllable magnetic domain wall step motor (thickness 30 nm, width of the zig-zag 200 nm, width of the nucleation pad 600 nm). Bottom: sequence of magnetic force microscopy images and micromagnetic configurations showing the injection and propagation of a domain wall under the action of external magnetic fields H_i, H_{up}, and H_{dw} directed as sketched in the figure. The dark and bright portions on the left and right of the injection pad are not DWs, but they are only due to the stray field at the ends of the pad itself.

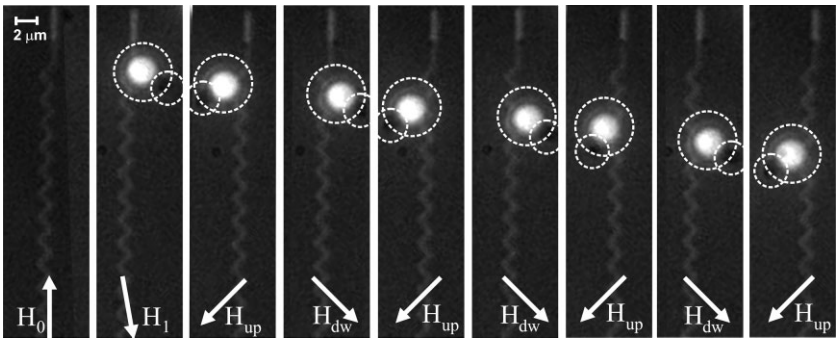

Figure 3. Sequence of fluorescence optical microscopy images (taken from video **M1**) showing the transport of a pair of magnetic beads, bound by chemical affinity between proteins initially loaded on them, in suspension above the zig-zag. The fluorescent bead (Dynabead, 2.8 μm diameter) is surface coated with anti-streptavidin and the dark bead is surface coated with streptavidin (Dynabead MyOne, 1 μm). The zig-zag is prepared in the initial state with a HH domain wall placed in the first corner of the zig-zag conduit (Fig. 2c). Then the sequence of fields H_{up} and H_{dw}, with duration of 100 μs, are applied to move the pairs of beads in suspension, after capture by a DW in the first corner of the zig-zag.

the non-magnetic binding between proteins and the chip surface due to hydrophobic interactions,[24] the device SiO_2 surface is blocked by 1% bovine serum albumine (BSA) preparated in phosphate buffered saline solution (PBS, Sigma-Aldrich, pH 7.4)containing 1% (v/v) Triton. Two suspensions, one containing 1 μm diameter beads coated with streptavidin and the other containing Cy3 fluorescent antibodies (anti-streptavidin-Cy3) covalently bound to the protein A coated 2.8 μm diameter beads, are prepared in external tubes. Then the two suspensions of beads are simultaneously flushed in the microfluidic cell placed inside a quadrupole electromagnet positioned over an inverted epifluerescence microscope, until a pair of beads (one fluorescent carrying the antibody and the other with streptavidin) is captured by the first HH DW, previously injected in the zig-zag structure by application of the sequence of fields H_0 and H_i.

The real-time movie M1 (see Supporting Information) and the corresponding sequence of frames reported in Figure 3, show the remotely controlled displacement of a pair of magnetic beads along the DW conduit by application of the same sequence of H_{up} and H_{dw} fields shown in Figure 2.

It is worth noting here that the time scale of DW motion in Py wires is very short, of the order of one ns over a length of a few micrometers,[14,16,18,19] while in our experiment the displacement of the magnetic particles is much slower (a few hundreds of milliseconds). In this sense the particles do not strictly move *with* the DW but rather follow it, with a drift motion superposed to Brownian motion towards the potential energy minimum generated at the new position occupied by the DW after the application of H. The speed of transport can be increased up to 15 $\mu m\,s^{-1}$, in our experimental conditions, and the bead finally released under the application of a field $-H_0$ (Fig. 2) along the nanostrip direction, which annihilates the DW while producing weaker stray fields in the tapered end of the zig-zag. This is shown in the real-time movie M2 (see Supporting Information), where the focus of the microscope is dynamically adjusted to follow the particle release. The direction of motion can be reversed at any time by reversing the direction of H_{up} and H_{dw} in sequence, so that it is possible to transport a molecule to a specific location of a microfluidic apparatus and bring it back to the initial position using the same conduit, after the desired reaction has been accomplished. It is also worth pointing out that the corners of the zig-zag are a stable position for the DW so that the proteins can be held in a selected position indefinitely, thus allowing further analysis.

A continuous control of the particle displacement at the nanoscale, synchronous to that of the coupled DW, can be achieved simply by modifying the nanostrip geometry, i.e., the potential landscape felt by a DW. This remarkable capability can be implemented using curved nanostrip structures, as illustrated in the next example for a 30 μm-diameter circular Py ring. Two DWs, one HH and the other TT, are initially generated in the ring by applying a saturating magnetic field H_0, as shown by the OOMMF micromagnetic simulations and MFM images in the top panel of Figure 4–1. Once created, the DWs can be moved around the circumference by the application of a smaller field H (Fig. 4–2 and 4–3). By rotating the field both the DWs are displaced with an angular speed equal to that of the rotating field, thus achieving a synchronous and fully controllable DW motion. The required magnitude is determined by the ring radius and the local DW pinning sites due to edge irregularities and material inhomogeneities as discussed below. The sequence of optical microscopy images in the bottom panel of Figure 4 shows two clusters of plain magnetic particles (nanomag-D, 500 nm diameter) in solution following the field induced displacement of the coupled DWs. The sequence of optical microscopy images in the bottom panel of Figure 4 (from the movie M3, see Supporting Information) shows two magnetic particles following the field-induced displacement of the coupled DWs. The continuity and reversibility of the motion of the particles can be appreciated looking at the movies M3 and M4 (see Supporting Information), the latter showing two adjacent rings with only one particle each, one at a HH DW and the other at a TT DW. By studying the motion of particles after rotation of the field by steps of 1° we verified that this geometry allows for the control of the displacement and positioning of a magnetic particle with a precision of 100 nm, as expected considering that the DW width is, in this case, about 100 nm. This is a crucial achievement in view of application to nanomanipulation of particles and molecules for fundamental investigations and synthesis.

Another peculiarity of our approach is that one or more sensors of DWs and magnetic particles described in a previous work[25–27] can be fully integrated in the system as they essentially consist in a portion of the DW conduit, e.g., a corner, flanked by conductive contacts for detecting electrically the presence of a DW thanks to the anisotropic magnetoresistance effect. Such a sensor can then be placed in the middle of a conduit and act as a magnetic particle counter, allowing for a digital control of the particles surfing on the conduits. In prospective, another advantage is represented by the possibility to realize complex networks of conduits, including crosses and bifurcations, where the motion of cells or molecules carried by magnetic beads can be remotely programmed and

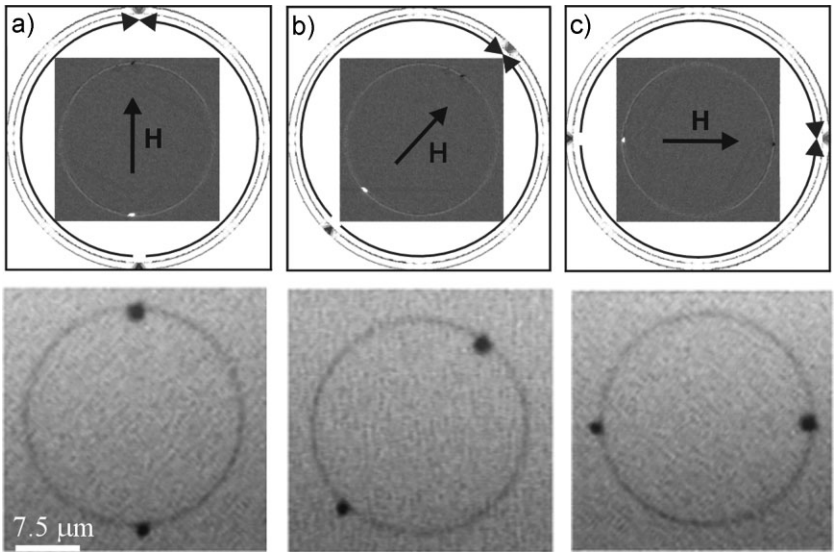

Figure 4. Top Panel: micromagnetic simulations and magnetic force microscopy images of the nucleation and displacement of HH and TT domain walls in a circular ring obtained by applying a rotating field H. Bottom panel: optical microscopy images (from movie **M3**) of the displacement of two magnetic particles captured by the two domain walls in a 30 μm diameter Py ring (thickness 30 nm, width 200 nm) by applying a rotating field H of 300 Oe. The continuous motion of two magnetic nanoparticles on two adjacent rings with smaller diameter (10 μm) is shown in the movie **M4** recorded with an optical microscope, available as Supporting Information.

controlled. This capability is unique compared to other technologies and pave the way to the realization of networks of conduits with externally programmable functions and continuous monitoring of the desired process.

In conclusion we demonstrated a novel method for on chip manipulation at the micro- and nanoscale of individual magnetic beads carrying biological entities, thanks to the interaction between them and DWs propagating in magnetic nanostrips. The approach described here allows for on-chip micro- and nanoscale-manipulation of biological entities, with a much lower degree of complexity compared to other methods.[29] The chip with the magnetic nanoconduits has been integrated in a microfluidic system where bead manipulation at the nanoscale is obtained simply by application of external magnetic fields. Many applications can be envisaged, ranging from the sorting of different biomolecules or cells labeled with different beads, to more complex processes of molecular analysis and synthesis in conduits networks containing bifurcations, intersections, straight and curved portions with a continuos remote control of the process. Finally, our approach paves the way to the realization of more fundamental experiments that could be carried out in parallel on different conduits patterned on the same chip, thus allowing the probing of statistical properties of biological systems.

Experimental

Nanostrips Fabrication and Geometry: Zig-zag conduits and circular rings are made of a 30 nm thick Permalloy strip e-beam lithographically patterned on top of a SiO_2/Si substrate, followed by the lift-off step and capped with a SiO_2 protecting layer 50 nm thick. The width of the Permalloy strip is 200 nm in both cases. For ziz-zag conduits the width of the injection pad is 600 nm and the length of each oblique segment is 2 μm. Circular rings have a diameter of 30 μm.

Micromagnetic Simulations: Micromagnetic simulations have been performed using the OOMMF public simulation platform [30]. The material parameters used for the simulations are those contained in the OOMMF program for Permalloy (viz., saturation magnetization $M_s = 860 \times 10^3\ A\,m^{-1}$, exchange stiffness constant $A = 1.3 \times 10^{-11}\ J\,m^{-1}$, no magnetocrystalline anisotropy has been considered; the damping coefficient used in the simulations is 0.5). We used a cubic cell of 5 nm side, which is slightly smaller than the exchange length of ~5.2 nm, defined as $\lambda_{ex} = \sqrt{(2A/\mu_0 M_S^2)}$.

Experiments on Magnetic Particle Manipulation: Figure 5 shows the setup used for the biological experiments in which a microfluidic cell is positioned at the center of a four coil electromagnet. Pulsed magnetic fields with duration of 100 μs in the case of the zig-zag conduits, or continuous rotating fields in the case of circular rings, are applied to move the beads under the objective of a microscope. The microfluidic cell, sketched on the top has been made of poly(methyl methacrylate) (PMMA), while optical access has been realized by bonding a microscope glass to the PMMA using waterproof tape.

For the manipulation of plain beads a solution of NH_4-OH (pH 8, 10^6 particles μL^{-1}) containing magnetic nanoparticles (nanomag-D, 500 nm diameter) has been flushed.

The fluorescence data was imaged by EMCCD camera (512 × 512 pixels, CascadeII, Photometrics) coupled to an inverted microscope (Nikon Eclipse TE2000-U) fitted with a 60× water immersion objective (N.A. 1.0, Nikon), FITC filter (Excitation: 465-495 nm, Dichroic: 505 nm, Emission: 515–555 nm, Nikon), and a 1.5× lens (Nikon). The fluorescence excitation illumination was provided to the microscope by a metal halide light source (200 W, Prior Lumen) via a liquid light guide. The

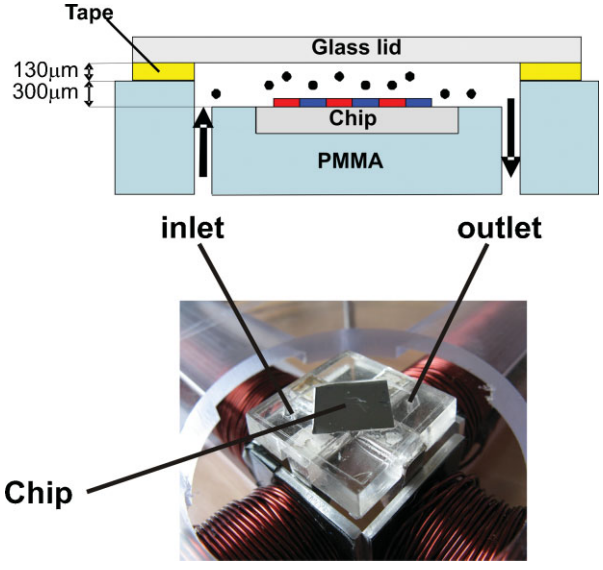

Figure 5. Top: Sketch of the microfluidic cell, where inlet and outlet are connected to syringe pumps. Bottom: The microfluidic cell inserted in the middle of the magnetic poles is slightly elevated with respect to the maximum field plane in order to exploit the field gradient to attract the particles on the chip surface.

measurements with plain beads on the circular structure were realized through a Leica Optical Microscope DMR with 100× objective.

Coupling of Proteins with Magnetic Beads: anti-streptavidin (Sigma-Aldrich) was labeled with Cy3 from GE Healthcare according to the standard protocol from the manufacture. Briefly, 10 mg of anti-streptavidin were added to the vial with Cy3 dye and incubated for 1 hour. Unreacted dye was separated from the anti-streptavidin-Cy3 using the PD-10 desalting column from GE Healthcare, columns were equilibrated with PBS containing 0.1% (v/v) NaN_3. Protein A modified magnetic beads (Dynabeads Protein A, Invitrogen) with 2.8 μm in diameter were coupled to the anti-streptavidin according to the protocol recommended by a manufacturer. 10 μg of antibodies in PBS (200 μL) with Triton 0.1% (v/v) and 1.5 mg beads were incubated with gentle rotation for 15 min at room temperature. After washing the bead-Ab complex were resuspended in PBS with 1% Triton and used for further experiments.

Acknowledgements

The authors thank B. T. Dalseet, L. H. Thandrup, R. Marie, F. G. Bosco, D. Chrastina for useful discussions, M. Leone for his skilful technical support. This work was partially funded by Fondazione Cariplo via the project SpinBioMed (Project No. 2008.2330). P.V. acknowledges funding from the Department of Industry, Trade, and Tourism of the Basque Government, the Provincial Council Gipuzkoa under the ETORTEK Program (Project No. IE06-172), the Spanish MICINN (Project CSD2006-53), and the EU VII Framework Programme (grant agreement No. PIEF-GA-2008-220166). M.F.H. acknowledges The Danish Council for Independent Research, Technology and Production Sciences. V.M. acknowledges support by the U.S. NSF, Grant ECCS-0823813. Supporting Information is available online from Wiley InterScience or from the author.

Received: January 13, 2010

[1] C. H. Chiou, Y. Y. Huang, M. H. Chiang, H. H. Lee, G. B. Lee, *Nanotechnology* **2006**, *17*, 1217.
[2] J. Dobson, *Nat. Nanotechnol.* **2008**, *3*, 139.
[3] D. L. Graham, H. A. Ferreira, P. P. Freitas, *Trends Biotechnol.* **2004**, *22*, 455.
[4] T. Deng, G. M. Whitesides, M. Radhakrishnan, G. Zabow, M. Prentiss, *Appl. Phys. Lett.* **2001**, *78*, 1775.
[5] C. S. Lee, H. Lee, R. M. Westervelt, *Appl. Phys. Lett.* **2001**, *79*, 3308.
[6] A. H. B. De Vries, B. E. Krenny, R. van Driel, J. S. Kanger, *Biophys. J.* **2005**, *88*, 2137.
[7] B. Yellen, G. Friedman, *Adv. Mater.* **2004**, *16*, 111.
[8] K. Gunnarsson, P. E. Roy, S. Felton, J. Pihl, P. Svedlindh, S. Berner, H. Lidbaum, S. Oscarsson, *Adv. Mater.* **2005**, *17*, 1730.
[9] R. S. Conroy, G. Zabow, J. Moreland, A. P. Koretsky, *Appl. Phys. Lett.* **2008**, *93*, 203901.
[10] L. E. Helseth, T. M. Fischer, T. H. Johansen, *Phys. Rev. Lett.* **2003**, *91*, 208302.
[11] P. Tierno, S. V. Reddy, M. G. Roper, T. H. Johansen, T. M. Fisher, *J. Phys. Chem. B* **2008**, *112*, 3833.
[12] R. Bertacco, M. Cantoni, M. Donolato, M. Gobbi, D. Petti, S. Brivio, P. Vavassori, Italian Patent Application No. VI2009A000026, (**2009**).
[13] R. D. McMichael, M. J. Donahue, *IEEE Trans. Magn.* **1997**, *33*, 4167.
[14] Y. Nakatani, A. Thiaville, J. Miltat, *Nat. Mater.* **2003**, *2*, 521.
[15] S. S. P. Parkin, M. Hayashi, L. Thomas, *Science* **2008**, *320*, 190.
[16] T. Ono, H. Miyajima, K. Shigeto, K. Mibu, N. Hosoito, T. Shinjo, *Science* **1999**, *284*, 468.
[17] D. A. Allwood, G. Xiong, M. D. Cooke, C. C. Faulkner, D. Atkinson, N. Vernier, R. P. Cowburn, *Science* **2002**, *296*, 2003.
[18] D. Atkinson, D. A. Allwood, G. Xiong, M. D. Cooke, R. P. Cowburn, *Nat. Mater.* **2003**, *2*, 85.
[19] G. S. D. Beach, C. Nistor, C. Knutson, M. Tsoi, J. L. Erskine, *Nat. Mater.* **2005**, *4*, 741.
[20] A. Yamaguchi, T. Ono, S. Nasu, K. Miyake, K. Mibu, T. Shinjo, *Phys. Rev. Lett.* **2004**, *92*, 077205.
[21] M. Kläui, C. A. F. Vaz, J. A. C. Bland, W. Wernsdorfer, G. Faini, E. Cambril, L. J. Heyderman, F. Nolting, U. Rüdiger, *Phys. Rev. Lett.* **2005**, *94*, 106601.
[22] P. Vavassori, V. Metlushko, B. Ilic, *Appl. Phys. Lett.* **2007**, *91*, 093114.
[23] D. A. Allwood, G. Xiong, C. C. Faulkner, D. Atkinson, D. Petit, R. P. Cowburn, *Science* **2005**, *309*, 1688.
[24] L.-E. Johansson, K. Gunnarsson, S. Bijelovic, K. Eriksson, A. Surpi, E. Göthelid, P. Svedlindh, S. Oscarsson, *Lab Chip* **2010**, *10*, 654.
[25] P. Vavassori, V. Metlushko, B. Ilic, M. Gobbi, M. Donolato, M. Cantoni, R. Bertacco, *Appl. Phys. Lett.* **2008**, *93*, 203502.
[26] M. Donolato, M. Gobbi, P. Vavassori, M. Leone, M. Cantoni, V. Metlushko, B. Ilic, M. Zhang, S. X. Wang, R. Bertacco, *Nanotechnology* **2009**, *20*, 385501.
[27] R. Bertacco, P. Vavassori, Italian Patent Application No. TO2008A000314, **2008**.
[28] G. Vieira, T. Henighan, A. Chen, A.J. Hauser, F.Y. Yang, J.J. Chalmers, R. Sooryakumar, *Phys. Rev. Lett.* **2009**, *103*, 128101.
[29] K. C. Neuman, A. Nagy, *Nat. Methods* **2008**, *5*, 491.
[30] M. J. Donahue, D. G. Porter, OOMMF User's Guide,Version 1.0. Interagency Report NISTIR 6376 (National Institute of Standards and Technology,Gaithersburg, **1999**,).